ICES Journal of Marine Science, 2023, Vol. 0, Issue 0, 1–14
https://doi.org/10.1093/icesjms/fsad190
Received: 4 April 2023; **revised:** 4 September 2023; **accepted:** 5 November 2023
Original Article

Overlap between the Mid-Atlantic Bight Cold Pool and offshore wind lease areas

Rebecca Horwitz [1,*], **Travis N. Miles** [1], **Daphne Munroe** [1,2], **Josh Kohut** [1]

[1]Department of Marine and Coastal Sciences, Rutgers University Center for Ocean Observing Leadership, 71 Dudley Rd, New Brunswick, NJ 08901, United States
[2]Rutgers the State University of New Jersey, Haskin Shellfish Research Laboratory, 6959 Miller Ave, Port Norris, NJ 08349, United States
*Corresponding author. Department of Marine and Coastal Sciences, Rutgers University Center for Ocean Observing Leadership, 71 Dudley Rd, New Brunswick, NJ 08901, United States. E-mail: bhorwitz@marine.rutgers.edu

Abstract

The Mid-Atlantic Cold Pool is a seasonal mass of cold bottom water that extends throughout the Mid-Atlantic Bight (MAB). Formed from rapid vernal surface warming, the Cold Pool dissipates in the fall due to mixing events such as storms. The Cold Pool supports a myriad of MAB coastal ecosystems and economically valuable commercial and recreational fisheries. Offshore wind energy has been rapidly developing within the MAB in recent years. Studies in Europe demonstrate that offshore wind farms can impact ocean mixing and hence seasonal stratification; there is, however, limited information on how MAB wind development will affect the Cold Pool. Seasonal overlap between the Cold Pool and pre-construction wind lease areas at varying distances from shore in the MAB was evaluated using output from a data-assimilative ocean model. Results highlight overlap periods as well as a thermal gradient that persists after bottom temperatures warm above the threshold typically used to identify the Cold Pool. These results also demonstrate cross-shelf variability in Cold Pool evolution. This work highlights the need for more focused ocean modeling studies and observations of wind farm effects on the MAB coastal environment.

Keywords: stratification; bottom temperature; Cold Pool; offshore wind; Mid-Atlantic Bight

Introduction

The Mid-Atlantic Cold Pool is a seasonal mass of cold bottom water extending throughout the Mid-Atlantic Bight (MAB) from Nantucket, Massachusetts to Cape Hatteras, North Carolina, resulting in one of the largest thermal gradients in the world. The MAB Cold Pool is present primarily between depths of 20–100 m (Bigelow 1933). This stratification and the associated cold bottom temperatures and nutrient-rich environment support a diverse coastal ecosystem, including economically important recreational and commercial fisheries (Miles et al. 2021). Although defined wind lease areas are in flux, as of 2023, within the MAB, over 2 million acres of the continental shelf have been leased for offshore wind energy projects that are under development, including sites that overlap with the seasonal Cold Pool (Miles et al. 2021, Musial et al. 2022, Methratta et al. 2023). Limited information exists about the extent of this overlap as well as the impact of these future wind turbines on the Cold Pool (Miles et al. 2021).

The Cold Pool develops in the winter as cold water from Nantucket Shoals, north of the MAB, is transported southward to well-mixed MAB water (Houghton et al. 1982, Ou and Houghton 1982). In the spring, as surface water temperature increases and storm frequency decreases, a strong thermocline develops that isolates this cold and relatively fresh bottom water known as the Cold Pool (Bigelow 1933, Houghton et al. 1982). Stratification within the MAB is controlled and stabilized by salinity and temperature (Castelao et al. 2010). The strength of the thermocline, driven primarily by temperature, reaches a seasonal peak between July and August (Castelao et al. 2010). As surface temperatures begin to decrease in the late summer and early fall, the thermocline weakens, and fall storms eventually mix warmed stratified surface waters to the bottom, dissipating the Cold Pool (Bigelow 1933, Houghton et al. 1982, Ou and Houghton 1982, Castelao et al. 2010, Lentz 2017, Chen et al. 2018). The seasonal interannual variability of the Cold Pool can be influenced by annual large-scale climate and oceanic processes such as increased upwelling conditions or more frequent storm events (Houghton et al. 1982, Glenn et al. 2004, Li et al. 2014, Chen et al. 2018; Chen and Curchitser 2020).

There is along-shelf variation of the Cold Pool within the MAB that defines three distinct regions: the northern MAB, the central MAB, and the southern MAB (Bigelow 1933, Castelao et al. 2010, Lentz 2017). The geography of the coastline along the Central MAB enhances the coastal upwelling response to summertime southerly winds (Castelao et al. 2010). The proximity to the Hudson River within the central MAB also changes the salinity within the Cold Pool in this region compared to the northern and southern MABs (Castelao et al. 2010). The Central MAB has the coldest bottom water during peak Cold Pool months (Ou and Houghton 1982, Castelao et al. 2010, Lentz 2017).

Seasonal Cold Pool evolution is integral to MAB ecosystem processes. Upwelling along the MAB occurs each summer, transporting Cold Pool waters further inshore and toward the surface near the coast, which can drive phytoplankton blooms (Glenn and Schofield 2003, Glenn et al. 2004, Xu et al. 2011). The presence of Cold Pool water allows species ranges to extend further south than would be anticipated by latitude, supporting many economically and culturally valuable finfish and

shellfish fisheries (Gabriel 1992, Lucey and Nye 2010, Murray 2016, Friedland et al. 2022). The Cold Pool can also impact hurricanes along the MAB by enabling ahead-of-eye center cooling through shear-induced mixing of the stratified water column (Glenn et al. 2016).

The USA is anticipated to become one of the largest offshore energy markets by 2030 with an estimated 2.4 million acres under lease and >2100 turbine foundations to be installed (Musial et al. 2022, Shields et al. 2022, Methratta et al. 2023). The MAB region leads the nation in proposed offshore wind energy projects with current regional offshore wind goals totaling >30 gigawatts (GW) of energy within the next decade (Musial et al. 2022, Methratta et al. 2023). European offshore wind energy has been developed extensively and can provide insight into possible interactions between turbines, physical oceanographic processes, and biological systems within the MAB, although there are key differences between the regions (Methratta et al. 2020). While still applicable, results from European studies are more representative of conditions in the MAB during relatively weakly stratified periods and do not represent Cold Pool conditions (Miles et al. 2021). Likewise, many European lease areas use smaller capacity turbines with different spacing, further adding to uncertainty about how relevant prior research is to MAB conditions (Methratta et al. 2020).

Wind turbines can directly impact hydrodynamics within and around wind farms through their underwater infrastructure and indirectly through changes in both the surface and atmospheric wind fields (van Berkel et al. 2020). Structure-induced friction and blocking from flow past cylindrical structures often form Von Kármán vortex streets, increasing the turbulence directly downstream of the turbine. In the context of the Cold Pool, this could lead to less stratified conditions (Miles et al. 2021). It is unclear what the effects will be on a highly stratified system like the MAB Cold Pool if the area of increased turbulence is expanded (Carpenter et al. 2016, van Berkel et al. 2020). Likewise, the extraction of atmospheric kinetic energy by turbines may be amplified by larger clusters of wind turbines, in turn reducing shear-driven forcing at the sea surface, decreasing horizontal velocities, and turbulent mixing within several kilometers of the wind site (Christiansen et al. 2022, Floeter et al. 2022, Golbazi et al. 2022). This could mean that within the MAB, offshore wind projects overlapping with the Cold Pool could strengthen stratification. However, recent MAB-specific modeling has illustrated a surface cooling effect due to the extreme height of the newer turbines proposed within the MAB wind farms (Golbazi et al. 2022), which could reduce stratification. North Sea-focused modeling studies have attributed lower dissolved oxygen concentrations to the potential strengthening of stratification and decrease in depth of the mixed layer due to wind wake generation and upwelling and downwelling dipoles (Daewel et al. 2022). The implications of offshore wind on the hydrodynamic features of the MAB require further study due to the key differences between the two regions such as the broader spatial extent of wind lease areas (WLAs), the weaker tidal strength, and increased storm frequency within the MAB versus Europe, as well as the technological differences in turbine design (Brunner and Lwiza 2020, Miles et al. 2021). In this paper, we evaluate the extent and cross-shelf variability of spatial overlap between pre-construction MAB WLAs and the Cold Pool. We specifically evaluate the overlap between the Cold Pool and the Bureau of Ocean Energy Management lease area call sites listed in Fig. 1. We evaluate the duration, strength, and variability of stratification where the Cold Pool overlaps with these sites within the MAB using output from a data-assimilative regional ocean model known as Doppio (López et al. 2020).

Methods

Data used in this study was simulated by the Doppio model, a Regional Ocean Modeling System (ROMS) application of the MAB and the Gulf of Maine (López et al. 2020, Wilkin et al. 2022). ROMS is a 3D hydrostatic terrain following a primitive equation model used extensively for coastal applications (Haidvogel et al. 2000, Shchepetkin and McWilliams 2005). Doppio is an implementation of ROMS with a uniform 7 km horizontal grid and 40 vertical sigma layers, covering the period of 2007–2021. It includes atmospheric forcing from National Centers for Environmental Prediction (NCEP) products, namely the North American Regional Reanalysis (NARR) (Mesinger et al. 2006) for the period of 2007–2013 and the North American Mesoscale (NAM) (Janjic et al. 2005) forecast model for 2014 and later. Boundary conditions are based on daily mean data taken from the Mercator Ocean system (Dre´villon et al. 2008) provided by Copernicus Marine Environment Monitoring Service (CMEMS) as well as the Oregon State University Tidal Prediction Software (OTPS) (Egbert and Erofeeva 2002) for harmonic tidal forcing of sea level and depth-average velocity along the open boundaries.

Additionally, Doppio uses 4-dimensional variational data assimilation (4D-Var) to obtain the best state estimate of the ocean within the domain. This includes assimilation of satellite sea surface temperature, sea surface height, HF-radar ocean surface currents, and all available *in situ* observations from the MARACOOS and NERACOOS regional associations of the US Integrated Ocean Observing System (IOOS) among other datasets (Wilkin et al. 2022). The output of Doppio used in this study spans from 2007 to 2021 and was generated by the Rutgers Ocean Modeling Group. Data were accessed in July 2023 from the THREDDS catalog of Doppio ROMS 15-year monthly reanalysis, as described in Wilkin and Levin (2022).

Metrics defining the presence and location of the Cold Pool area where the vertical temperature gradient is 0.2°C/m or greater and the bottom temperature is 10°C or less (Houghton et al. 1982, Mountain 2003, de Boyer Montégut et al. 2004, Brown et al. 2012, Li et al. 2015, Lentz 2017, Miles et al. 2021). The density stratification over the MAB region is primarily thermally controlled during the peak Cold Pool months; thus, stratification is determined by calculating the temperature gradient:

$$0.2^{\circ}C/m \leq \delta T/\delta z \,\&\, T \leq 10^{\circ}C \quad (1)$$

All 25 active WLAs within the MAB were analyzed in this study to determine the seasonal and cross-shelf overlap, more specifically with the Cold Pool. Total surface area of the Cold Pool and the MAB WLAs was extracted using ArcGIS and further analyzed (BOEM 2023). The centroid of each of the 25 MAB WLAs was used as the study location for each WLA (Fig. 1). Single points were used because the size of each WLA is small relative to the resolution of Doppio (7 km). Study locations were divided into three MAB segments based on the physical characteristics of each region: north, central,

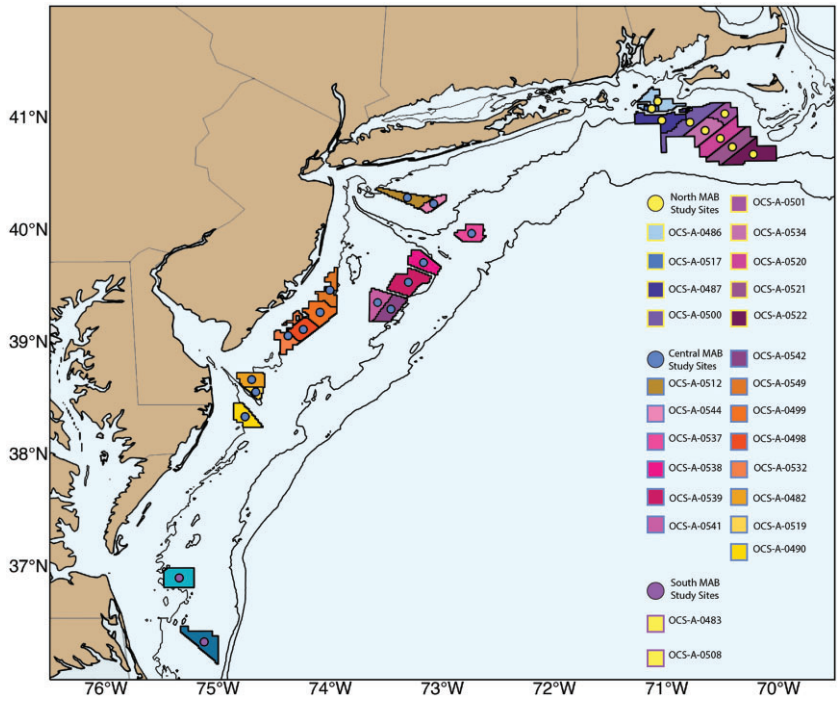

Figure 1. Study locations are depicted with circles and associated wind lease areas (WLAs) are shown as colored blocks, with colors indicating different lease blocks. The 25, 50, and 75 m isobaths are shown in black lines. Northern MAB sites correspond to the yellow circles with the lease blocks outlined in yellow. For northern MAB sites, blue hues represent nearshore sites (<43 m) and purple hues represent offshore sites (<43 m). Central MAB sites correspond to the blue circles with the lease blocks outlined in blue. For central MAB sites, yellow hues represent nearshore sites (<33 m) and pink hues represent offshore sites (<33 m). Southern MAB sites correspond to the purple circles with the lease blocks outlined in purple. The legend is organized from north to south.

and south (Bigelow 1933, Castelao et al. 2010, Lentz 2017). Within the central and northern MAB regions, study sites were further categorized into nearshore and offshore based on the average of the deepest and shallowest depths within each section. For northern MAB WLAs, the defined depth threshold is 43 m, and for central MAB WLAs, the defined depth threshold is 33 m. The southern MAB only has two WLAs, which we evaluate individually; hence, depth categorization was unnecessary. For each of these 25 study locations, the above method was used to determine the 15-year ensemble monthly averages of bottom temperatures and vertical temperature gradients, as well as standard deviations for variability across the 15-year span for each month for both criteria. Thermal gradients for each of the selected study sites were further evaluated by plotting monthly temperature-depth profiles.

Results

The MAB bottom temperatures warm from south to north and inshore to offshore, with the earliest warming along the southern and nearshore MAB regions (Fig. 2). By April, MAB areas south of New Jersey have already reached bottom temperatures above 10°C. Despite a northward bottom temperature warming trend through peak Cold Pool months, the area offshore of the New York Bight, near the Hudson Shelf Valley, remains below 8°C, even when more northern sites reach bottom temperatures close to 12°C (Fig. 2). The setup of the stratification (vertical thermal gradient values above 0.2°C/m) within the MAB is much less uniform (Fig. 3). In contrast to bottom temperature warming, stratification setup initiates in the north; however, the setup is much faster across all depths and latitudes within the MAB (Fig. 3). Reduction of stratification occurs earliest offshore and moves inshore during the later summer months (Fig. 3).

The combined stratification and bottom temperature metrics show that the Cold Pool sets up earliest at the southern edge of the MAB nearshore around North Carolina (Fig. 4). The Cold Pool remains inshore of the 50-m isobath during April and begins to set up in the NY bight at the mouth of the Hudson Shelf Valley and initiation of the Hudson Shelf Valley following stratification setup seen in Fig. 3. By May, the Cold Pool dissipated south of Delaware from warming bottom temperatures but extended northward to Massachusetts and offshore to depths of 100 m (Figs 2 and 4). Following the trend of warming bottom temperatures seen in Fig. 2, the Cold Pool weakens fastest inshore, leaving only a spatial footprint of cold bottom waters along the New York Bight in September (Figs 2 and 4).

For the central MAB WLAs, bottom temperatures within the MAB warm more rapidly nearshore than offshore (Fig. 2). Within the nearshore WLAs, bottom temperatures reach well above 10°C between April and May, while bottom temperatures in the offshore WLAs do not reach 10°C until July (Fig. 2). Nearshore, maximum bottom temperatures exceed 20°C, while the offshore bottom temperatures reach a maximum of 16°C (Fig. 2). A stratified water column (the temperature gradient is above 0.2°C/m) also forms earlier in nearshore WLAs than offshore WLAs, with nearshore values close to 0.6°C/m by April (Fig. 3). However, stratification is sustained for longer in offshore sites, with temperature gradients maintained above 0.2°C/m through September (Fig. 3).

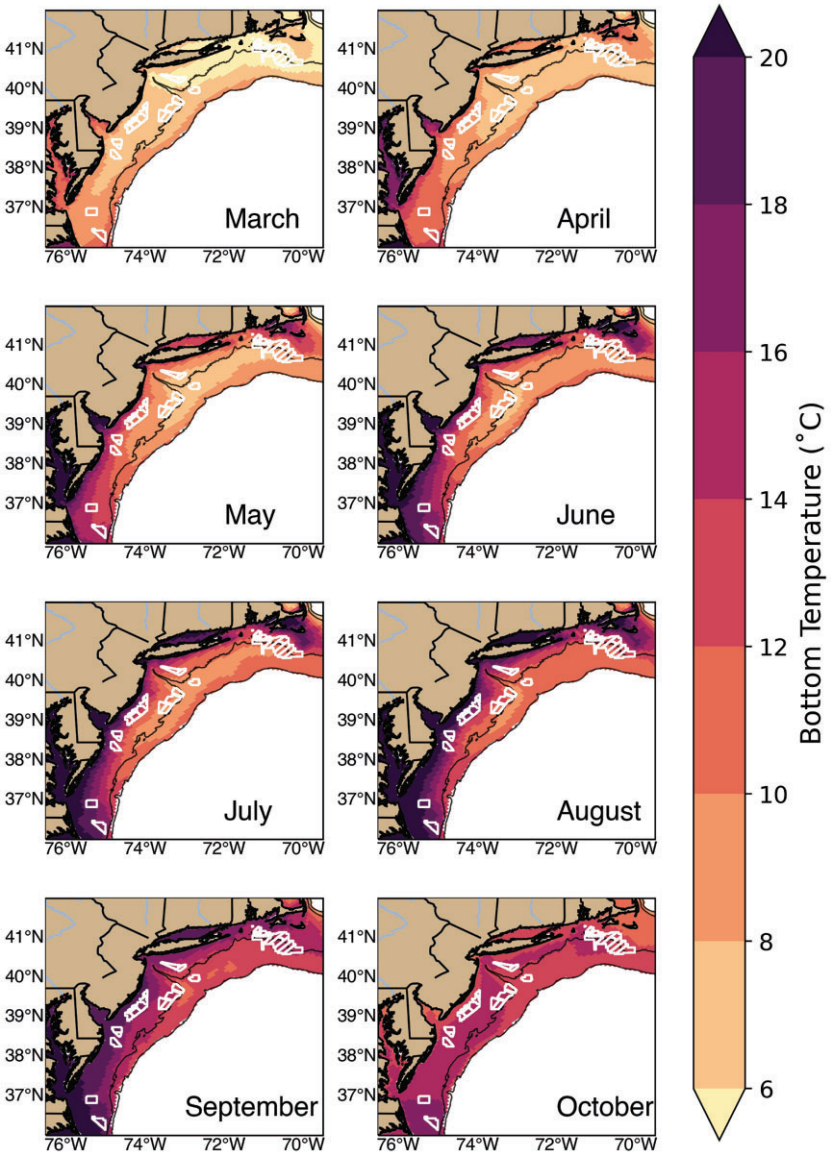

Figure 2. Monthly averaged bottom temperatures based on Doppio simulations spanning 2007 to 2021 within the MAB. Only peak Cold Pool months are included. The Cold Pool bottom temperatures are defined herein as those below the 10°C threshold. WLAs included in this study are outlined in white. The 50 and 100 m isobaths are shown in black.

Throughout peak Cold Pool months, the overlap between MAB WLAs and the Cold Pool varies substantially (Fig. 4). In the month of March, despite the Cold Pool's surface area of 1109 km^2, there is no overlap with the MAB WLAs (Fig. 4). In the month of April, the surface area of the Cold Pool expanded to 19 595 km^2 (Fig. 4). 19% of the MAB WLAs overlapped with the Cold Pool in April, although only 9% of the Cold Pool was covered by MAB WLAs (Fig. 4). In May, the Cold Pool surface area peaked at 56 153 km^2, and the MAB WLAs overlap with the Cold Pool increased to 81%, the highest annual overlap. Despite this large overlap, only 13% of the May Cold Pool was covered by MAB WLAs (Fig. 4). In June, the Cold Pool surface area covered 50 787 km^2, and 62% of the MAB WLAs overlapped (Fig. 4). Only 11% of the June Cold Pool was covered by the MAB WLAs (Fig. 4). In July, the Cold Pool surface area decreased to 36 942 km^2, and 41% of the MAB WLAs overlapped with 10% of the Cold Pool covered by the WLAs (Fig. 4). August is the last month of significant overlap between the Cold Pool and WLAs. The surface area of the August Cold Pool decreased to 19 333 km^2 with only 18% of the Cold Pool covered by WLAs and only 8% of WLAs overlap (Fig. 4). September was the only month that had a larger percentage of WLAs overlap with the Cold Pool (0.3%) than the percentage of the Cold Pool covered by WLAs (0.1%) (Fig. 4).

There are limited latitudinal differences in the duration and strength of the Cold Pool based on both metrics across the nine northern WLAs. Four of the northern MAB sites are nearshore with depths shallower than 43 m. The offshore sites (the remainder of the northern WLAs) are at ~50 m depth (Fig. 1). All eight northern MAB WLAs had stratification strength reach 0.2°C/m in the month of May while maintaining the bottom temperature below 10°C, signifying the presence of the Cold Pool starting in May (Fig. 5). The four nearshore sites had bottom temperatures warm above 10°C

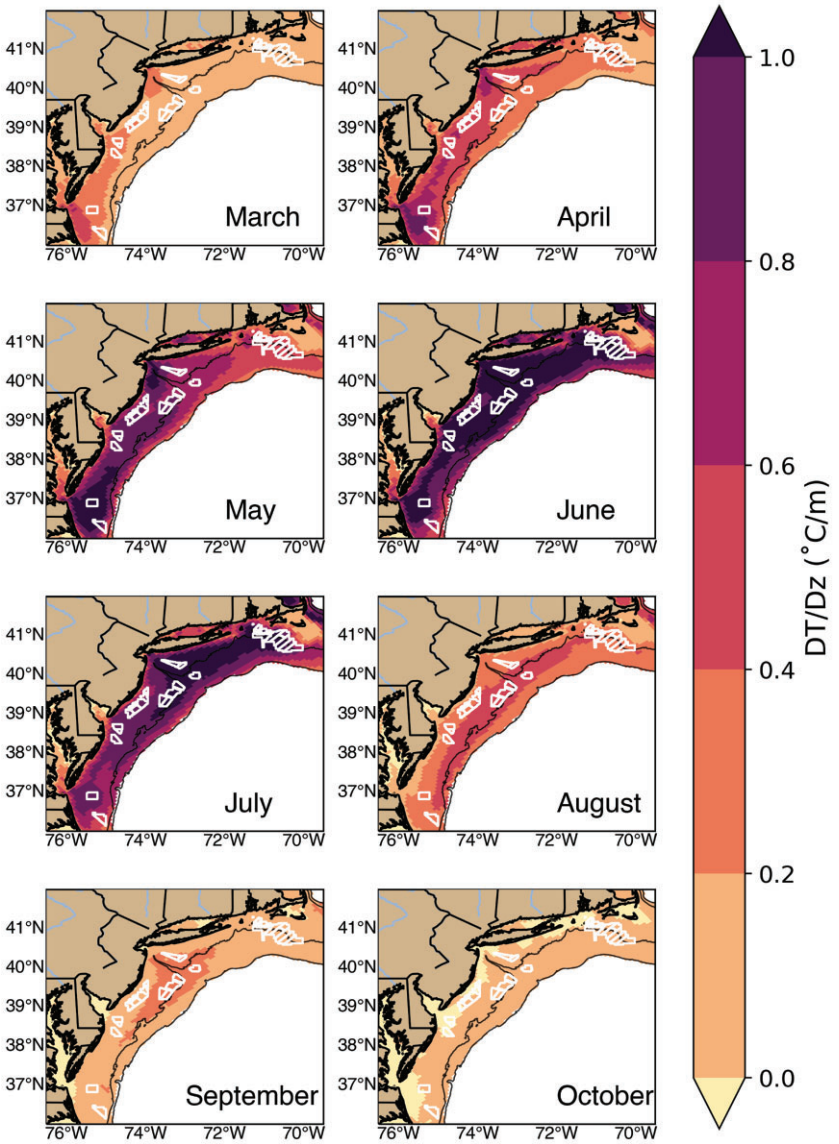

Figure 3. Monthly averaged temperature gradient values (dT/dz [°C/m)] based on Doppio simulations spanning 2007 to 2021 within the MAB. Only peak Cold Pool months are included. Cold Pool stratification is defined herein as dT/dz > 0.2°C/m. WLAs included in this study are outlined in white. The 50 and 100 m isobaths are shown in black.

in the month of June, while the four offshore sites had bottom temperatures warm above the Cold Pool threshold in the month of July (Fig. 5).

Despite the difference in duration of the Cold Pool of one month versus two between the nearshore and offshore sites within the northern MAB, the evolution of the stratification strength and bottom temperatures between the groups was not noticeably different. All eight sites had thermal gradients peak in July at between 1 and 1.5°C/m, despite the faster warming of bottom temperatures within the four nearshore sites (Fig. 5). Even with the rapid warming of the bottom temperature above 10°C, in all eight MAB sites, the stratification strength remained above 0.2°C/m until September (Fig. 5). In all eight northern MAB sites, the minimum bottom temperature occurred well before the stratification strength reached 0.2°C/m in either March or February (Fig. 5). The maximum bottom temperature occurred in October in all eight sites (Fig. 5).

Thermal gradients for each of the northern selected study sites were further evaluated by plotting monthly temperature-depth profiles. In peak Cold Pool months, the vertical temperature gradient is similar between all study sites, despite the differences in depth and distance from shore (Fig. 6). Surface water temperature variability was relatively low across all eight sites with a 2°C difference throughout peak Cold Pool months.

Latitudinal differences can be seen in the duration and strength of the Cold Pool based on both metrics across the 14 central MAB study locations. The six central MAB offshore study locations are below 33 m of water depth, while the eight nearshore sites are <33 m of depth (Fig. 1). All six offshore study locations had bottom water temperatures below 10°C and a thermal gradient >0.2°C/m in the month of May, signifying the presence of the Cold Pool (Fig. 7). The bottom temperature at five of these offshore study points exceeded 10°C in August, meaning the Cold Pool duration there was

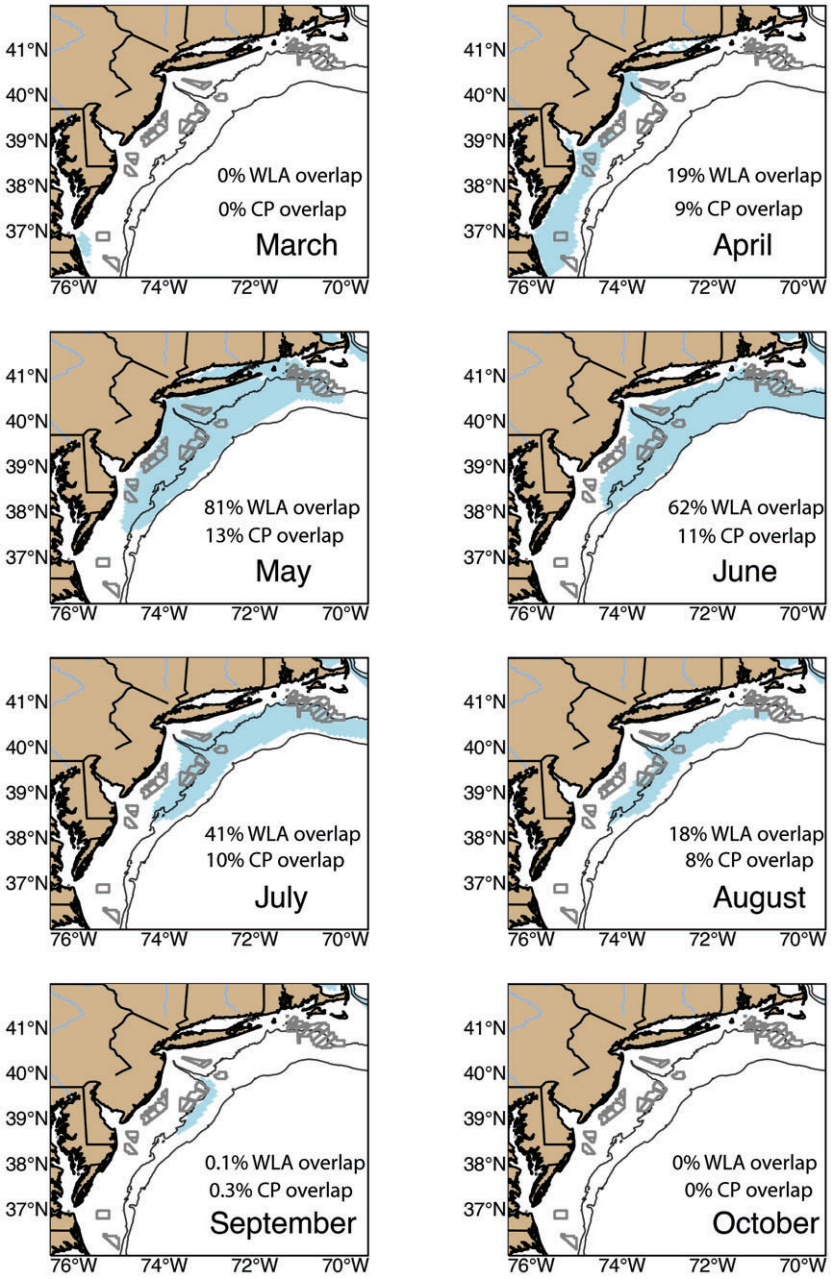

Figure 4. The Cold Pool is present in the areas of the shelf shaded in blue, which represent both bottom temperatures below 10°C and temperature gradients >0.2°C/m. Calculations were made based on Doppio simulations spanning 2007–2021 within the MAB. Only peak Cold Pool months are shown. Wind lease areas included in this study are outlined in gray. The 50- and 100-m isobaths are shown in black. Wind Lease Area Overlap with the Cold Pool (WLA overlap) and Cold Pool Covered by Wind Lease Areas (Cold Pool Overlap) percentages in km^2 are listed for each month in each panel.

approximately three months (Fig. 7). Despite the warming bottom temperatures in all six offshore sites, stratification above 0.2°C/m was maintained for three additional months dissipating in October (Fig. 7). Peak thermal gradient values occurred in July for all six offshore WLAs (Fig. 7). The highest bottom temperatures occurred as stratification broke down around October or November, consistent with downward mixing of warm surface waters due to fall transition storms.

There are notable differences in the Cold Pool evolution between the nearshore and offshore WLAs. In the eight central MAB nearshore, Cold Pool duration was shorter, spanning approximately one month, starting in April with increasing stratification and ending in May when the bottom temperature surpassed 10°C (Fig. 7). Despite the short duration of the Cold Pool, high thermal gradient values (>0.2°C/m) in these eight nearshore sites lasted for six months, dissipating in September (Fig. 7). Like the central MAB offshore WLAs, thermal gradients peaked at the nearshore sites in July. Despite an earlier development of stratification at the nearshore sites, the thermal gradient weakened at approximately the same time as the offshore sites (Fig. 7). Bottom temperatures reached a greater maximum value at the nearshore sites by >3°C (Fig. 7). Peak thermal gradient values were relatively similar between the central MAB nearshore and offshore WLAs.

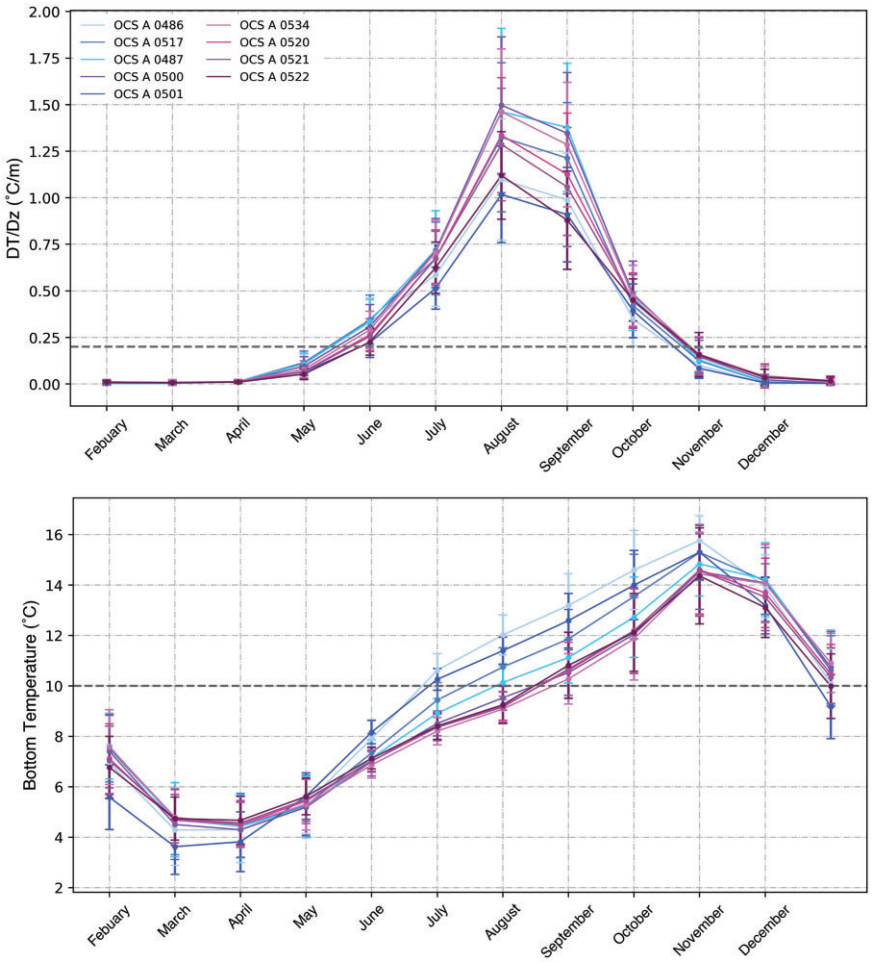

Figure 5. Monthly average bottom temperature (lower panel) and dT/dz values (upper panel) from 2007–2021 for northern MAB study locations based on Doppio simulations. Colors correspond to the specified wind lease area shown in Fig. 1. The Cold Pool exists when bottom temperatures remain below the dashed gray line and dT/dz values are above the above gray dashed line. Error bars show the standard deviation of variability for each month between 2007 and 2022. Blue hues represent nearshore sites (<43 m) and purple hues represent offshore sites (<43 m).

Thermal gradients for each of the selected central MAB study sites were further evaluated by plotting monthly temperature-depth profiles. In peak Cold Pool months, the vertical temperature gradient is similar between all study sites, despite the differences in depth and distance from shore (Fig. 8). Surface temperatures across all six sites differed the most in May and June with 3°C differences among sites. The difference in surface water temperature between sites decreased across Cold Pool months, while the difference in bottom temperatures increased, with a maximum difference in September of around 7°C between nearshore and offshore sites (Fig. 8). During July and August, surface temperatures at the nearshore sites were cooler and bottom temperature warmer than those of the offshore sites. The vertical temperature gradient values at the nearshore and offshore sites were similar, despite differences in depth and bottom temperatures.

Based on bottom temperature and stratification thresholds, the Cold Pool is only present in one of the two southern MAB WLAs, OCS-A-0483. Despite the presence of the Cold Pool according to the thresholds defined, the bottom temperature warms above 10°C within the same month that the stratification reaches 0.2°C/m for OCS-A-0483, meaning the Cold Pool presence is limited to one month (Fig. 9). Even with the warm bottom temperatures for both southern MAB WLAs, the stratification strength does reach 0.2°C/m and remains above the Cold Pool thermal gradient threshold until September for both sites (Fig. 9). Even in the southern MAB site, where the Cold Pool, according to the thresholds given, is not present, the bottom temperature reaches below 10°C. Not, however, simultaneously with the thermal gradient reaching 0.2°C/m. Both sites have peak thermal gradients in the month of June and maximum bottom temperatures warmer than the other two MAB regions. Based on the temperature profiles for the southern MAB WLAs, it is clear that the region does not have the same stratification strength as the northern and central MAB WLAs (Fig. 10).

Discussion

Regional Cold Pool trends offshore of New Jersey in this study are consistent with those of previous studies that discuss the spatial and temporal variability of the Cold Pool (Houghton et al. 1982, Ou and Houghton 1982, Mountain 2003, Castelao et al. 2010, Brown et al. 2012, Lentz 2017, Chen et al. 2018). Our work provides additional

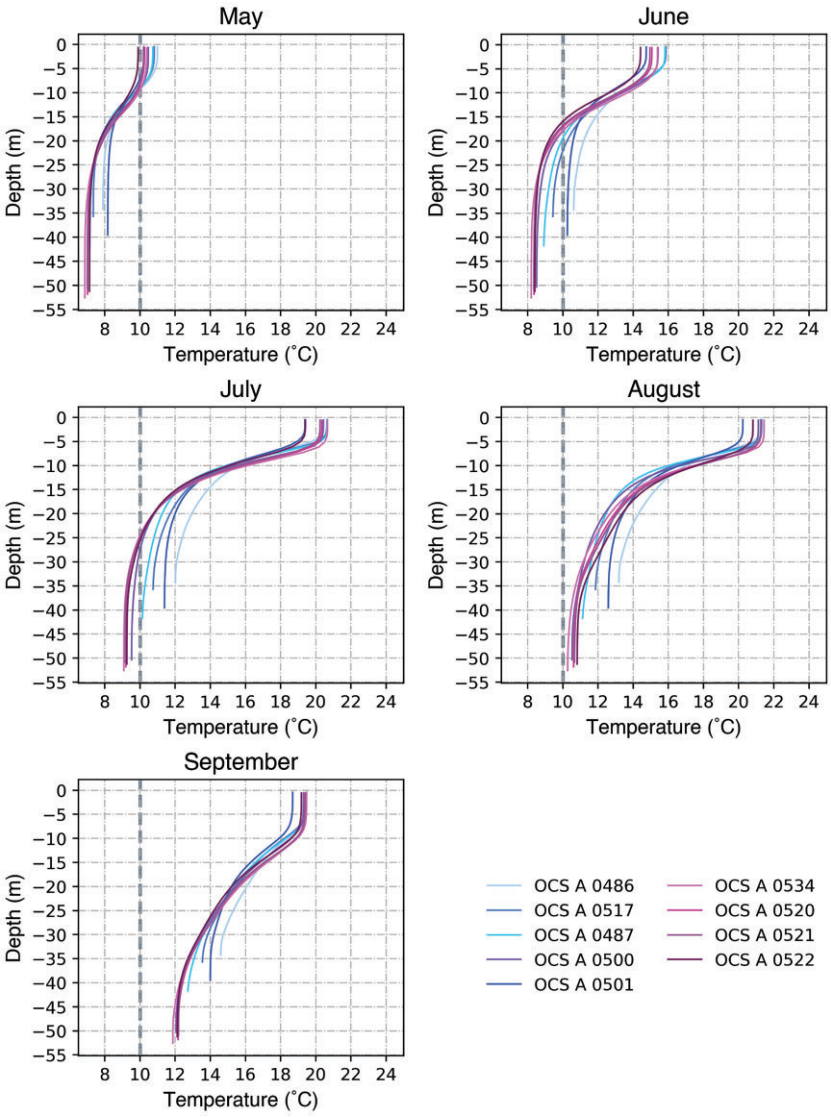

Figure 6. Northern MAB WLAs temperature profiles for Cold Pool months based on monthly averaged Doppio simulations from 2007 to 2021. Cold Pool bottom temperature threshold is depicted with the gray dashed line. The color of each profile corresponds to a study point within the selected wind areas shown in Fig. 1. Blue hues represent nearshore sites (<43 m) and purple hues represent offshore sites (<43 m).

context related to the co-location of this essential ocean feature and WLAs, but we provide some general comparisons with their results. Lentz (2017) utilizes observational data from the National Center for Environmental Information (NCEI) World Ocean Database, generally between 1955 and 2014 (Boyer et al. 2013), while Chen et al. (2018) are based on modeling results from a regional ROMS model that covers 1958–2007. While the DOPPIO model configuration has similarities to Chen et al. (2018), DOPPIO is a data-assimilative ocean model that benefits from both the extensive observations throughout the region and continuous spatial and temporal coverage of a modeling system. Generally, nearshore bottom temperatures warmed more quickly than offshore, which is consistent with previous results (Lentz 2017, Chen et al. 2018). However, we found that the bottom temperatures within the regional MAB were warmer than those reported in previous studies, accompanied by higher temperature gradients (Lentz 2017). Generally, the Cold Pool is shorter in duration at areas of shallower depths (Lentz 2017, Chen et al. 2018). These differences could be a result of the differing time periods between DOPPIO and the observations and models used in Lentz (2017) and Chen et al. (2018), as the Cold Pool has undergone significant warming over the last 40 years (Friedland et al. 2022). Previous studies have defined Cold Pool dissipation as the decrease in stratification strength in early fall from increased mixing by storm events and warming bottom temperatures (Lentz 2017, Chen et al. 2018). While findings in this study support the strengthened thermal gradient extending into the early fall, bottom temperatures at our study locations were consistently above accepted Cold Pool thresholds after May depending on the region. The thermal gradient in the central MAB has been observed to be greater than in other areas of the MAB, which is consistent with previous work (Lentz 2017, Chen et al. 2018). These previous studies indicate the maximum temperature gradients are between 0.5 and 0.8°C/m (Lentz 2017, Chen et al. 2018), while in both offshore and nearshore sites in this study they exceeded 1°C/m.

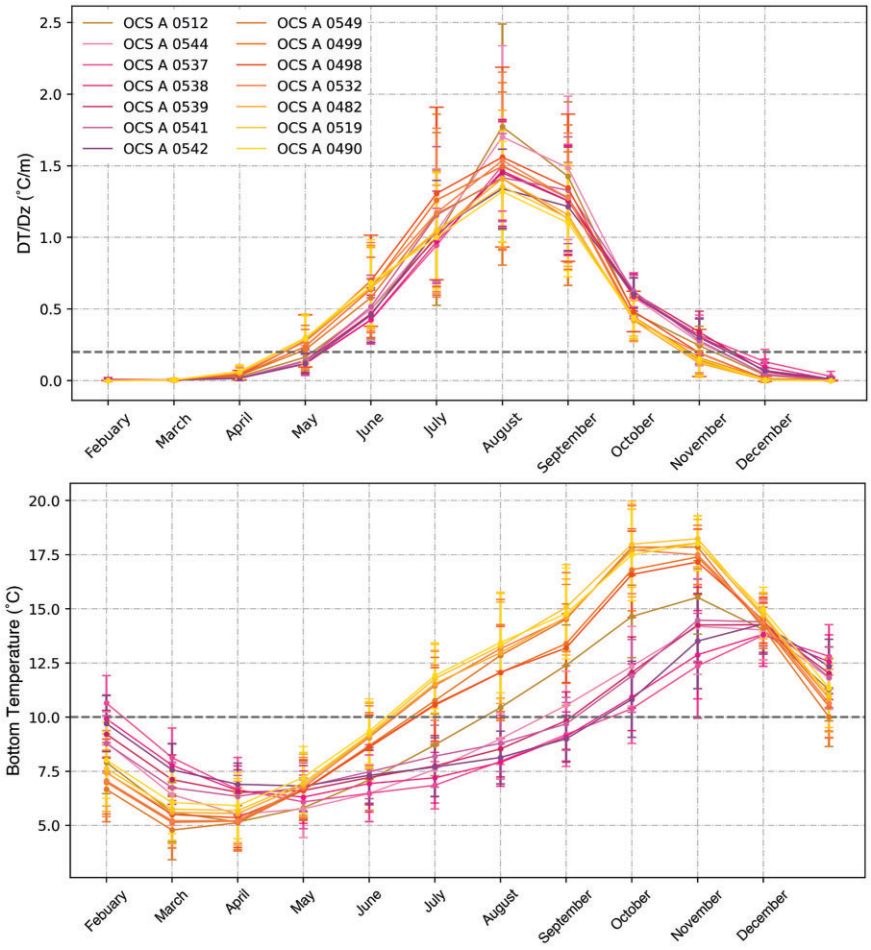

Figure 7. Monthly average bottom temperature (lower panel) and dT/dz values (upper panel) from 2007 to 2021 for central MAB study locations based on Doppio simulations. Colors correspond to the specified wind lease area shown in Fig. 1. Yellow hues represent nearshore sites (<33 m) while pink hues represent offshore sites (<33 m). The Cold Pool exists when bottom temperatures remain below the dashed gray line and dT/dz values are above the above gray dashed line. Error bars show the standard deviation of variability for each month between 2007 and 2022.

Cold Pool breakdown criteria have previously identified as bottom temperatures warming above 10°C and weakening of the thermal gradient below 0.2°C/m (Houghton et al. 1982, Lentz 2017, Chen et al. 2018); however, we found that the vertical thermal gradient remains above 0.2°C/m well beyond the time of bottom temperature warming above 10°C. Even at the nearshore sites where higher maximum vertical thermal gradient values are observed, stratification extends months after the bottom temperature warms. Stratification is the buoyancy force that inhibits mixing by flow past structures such as wind turbines, and it maintains ecologically important habitat (Miles et al. 2021). Atlantic Surf clams, Ocean Quahogs, and Sea Scallops are among the most economically valuable fisheries within the MAB region (Munroe et al. 2016, Powell et al. 2020, Miles et al. 2021, Friedland et al. 2022). These species are thermally sensitive and their distribution is often an indicator of changing bottom temperatures (Powell et al. 2020, Friedland et al. 2022). A 2023 study found that 20% of 177 species of MAB forage fish preferentially used habitat within WLAs (Friedland et al. 2023). Changes in stratification that have the potential to affect primary productivity may heavily impact these ecologically important species (Daewel et al. 2022, Friedland et al. 2023). Other demersal fish, such as the Yellowtail Flounder, use the changing bottom temperatures to trigger important life-stage changes (Sullivan et al. 2005, Sackett et al. 2008). Thermal gradients, changes in bottom temperature, and consequent changes in primary productivity could directly impact these and other commercially and ecologically important species in the region. Climate change has been warming waters within the MAB region in recent years, more specifically bottom temperatures (Wallace et al. 2018, Friedland et al. 2022, Amaya et al. 2023). Despite these warming temperatures, stratification associated with the Cold Pool has maintained values at and above 0.2°C/m. While 10°C is a useful indicator, these warming bottom temperatures may necessitate an updated bottom temperature threshold range. Because of the ecological and environmental importance of the Cold Pool, several metrics, in addition to bottom temperature, should be used to evaluate the Cold Pool.

This study shows a larger spatial and temporal overlap between the Cold Pool and WLAs further offshore versus wind lease areas closer to shore. We observed in this study that the average variation from 2007–2021 in Cold Pool metrics was limited for both bottom temperatures and stratification. Despite limited decadal Cold Pool variation, previous

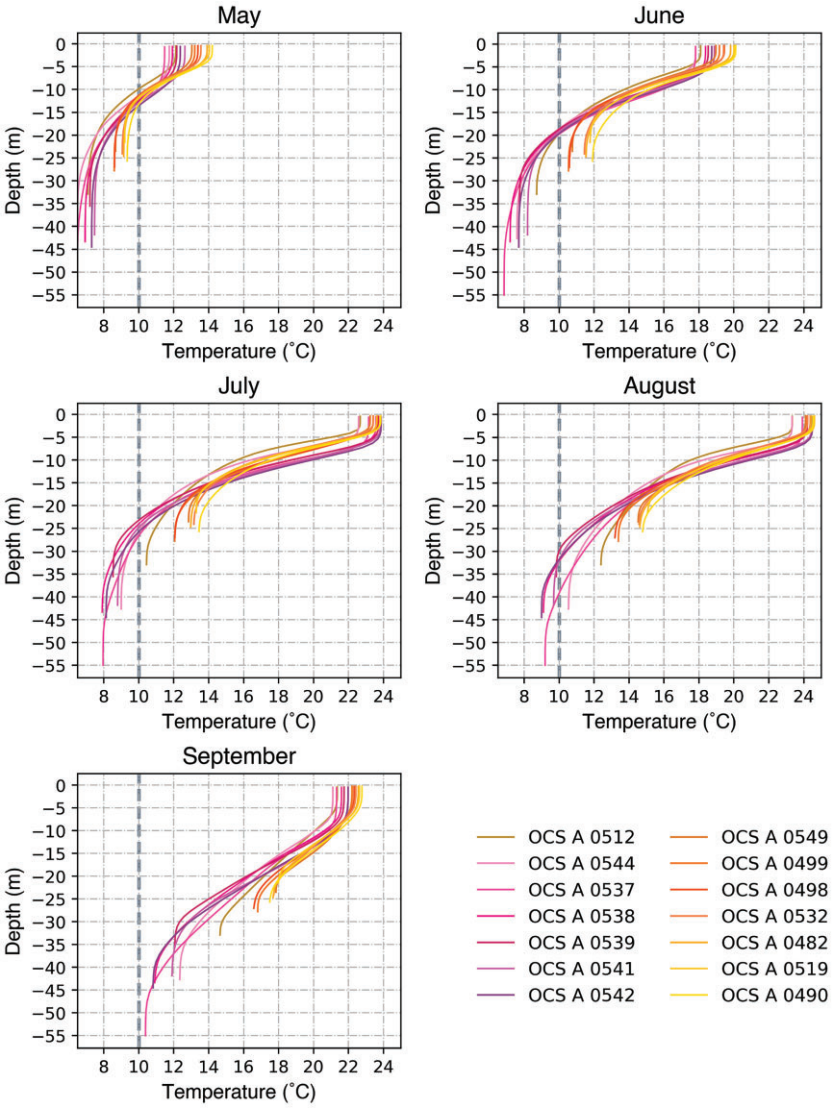

Figure 8. Central MAB WLAs temperature profiles for Cold Pool months based on monthly averaged Doppio simulations from 2007 to 2021. Cold Pool bottom temperature threshold is depicted with the gray dashed line. The color of each profile corresponds to a study point within the selected wind areas shown in Fig. 1. Yellow hues represent nearshore sites (<33 m), while pink hues represent offshore sites (<33 m).

studies have shown that broader ocean processes such as favorable upwelling or downwelling conditions can influence the daily and weekly variability of the Cold Pool (Houghton et al. 1982, Glenn et al. 2004, Li et al. 2014, Chen et al. 2018, Chen and Curchitser 2020). While we observed that there is limited overlap between the Cold Pool and MAB WLAs on a decadal time scale, daily variation in bottom temperatures and stratification can impact this overlap. Future work should evaluate short-term Cold Pool spatial variability to further increase certainty in WLAs overlap with this important regional feature.

Studies focused on European wind farms have shown that wind farms alter the hydrodynamic features of coastal environments (Carpenter et al. 2016, van Berkel et al. 2020, Christiansen et al. 2022, Floeter et al. 2022). These impacts depend heavily on the spatial extent of the wind farms as well as the temporal and spatial variability of stratification and mixing (Carpenter et al. 2016, Christiansen et al. 2022, Daewel et al. 2022). The current WLAs within the German Bight occupy a smaller area of the ocean than those proposed along the MAB. The stratification within the German Bight at depths <50 m is quantified as a 5–10°C difference between surface and bottom water temperatures, and tidal currents in this region can reach near 1.0 m/s (Carpenter et al. 2016, Christiansen et al. 2022). At the peak of thermal stratification in the German Bight during the year 2014, the bottom water temperature along the 40-m isobath only reached 14°C, resulting in a maximum thermal gradient of 0.35°C/m (Carpenter et al. 2016). During the years 2004–2013 along the 35 m isobath within the German Bight, the highest thermal gradient value was 0.37°C/m in July 2009 (Carpenter et al. 2016). The minimum peak thermal gradient value was 0.17°C/m in August 2004 (Carpenter et al. 2016). The maximum MAB thermal gradient value for the nearshore MAB sites, at a depth of ∼30 m in the central region was 1.77°C/m. The maximum stratification within the nearshore MAB sites was close to five times that of the Ger-

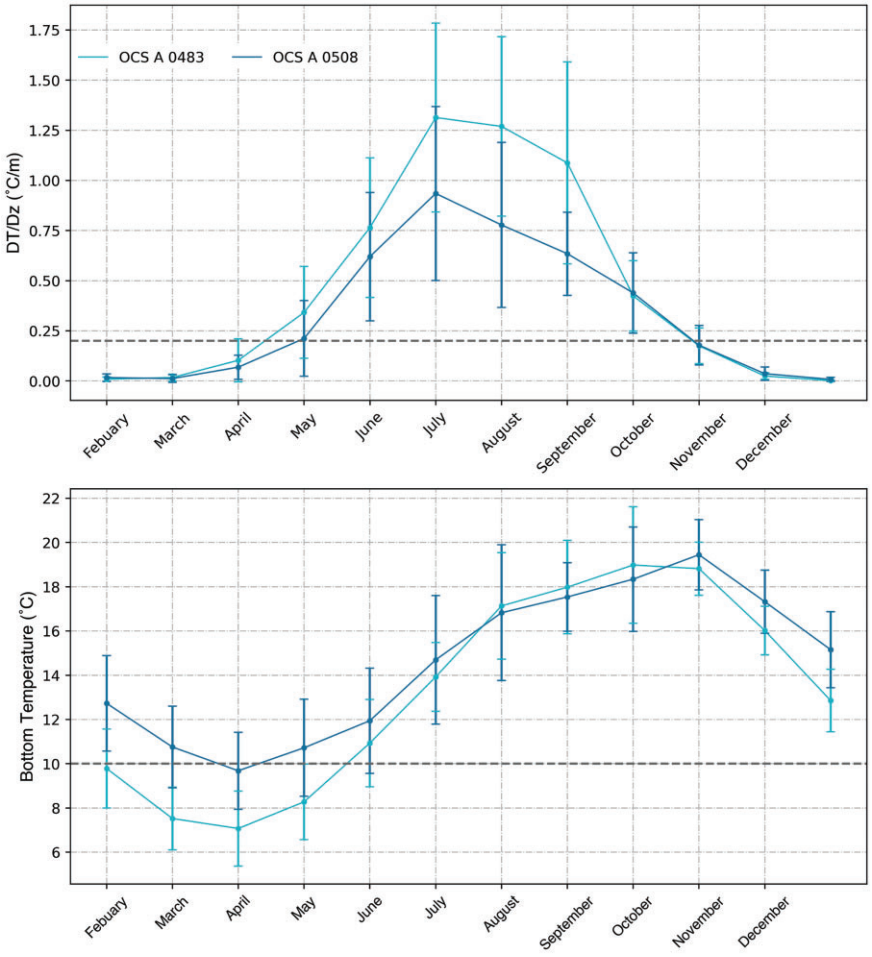

Figure 9. Monthly average bottom temperature (lower panel) and dT/dz values (upper panel) from 2007 to 2021 for southern MAB study locations based on Doppio simulations. Colors correspond to the specified wind lease area shown in Fig. 1. The Cold Pool exists when bottom temperatures remain below the dashed gray line and dT/dz values are above the above gray dashed line. Error bars show the standard deviation of variability for each month between 2007 and 2022.

man Bight. Local tidal forcing within the MAB is much weaker than the German Bight (>0.1 m/s), while storms are more frequent within the MAB (Brunner and Lwiza 2020). The German Bight, consequently, has considerably weaker stratification and stronger currents than the MAB during peak stratification times. Because of the spatial, technological, and environmental differences between the German Bight and the MAB, studies of the hydrodynamic impacts of wind farms in the German Bight cannot be directly extrapolated to the MAB Cold Pool. In November, when storm occurrences become more frequent within the MAB, the weakened stratification might lead to additional impacts from wind farms. The strength of stratification within the MAB and the findings of this study suggest that impacts from turbines on stratification may be less than those found in the German Bight. New studies (Friedland et al. 2023) have indicated that there is significant overlap between MAB forage fish and WLAs; however, the biological responses of the system to changes in habitat from extensive sandy benthic habitats to increased hard structure and intertidal remain unknown. New analyses are currently underway utilizing the methods proposed by Carpenter et al. (2016), but with the MAB stratification conditions. Additionally, more detailed simulations and pre- and post-construction observations should be further explored to fully capture the potential impacts of the turbine structure on the MAB Cold Pool. Our study highlights times and regions of overlap between MAB WLAs and the Cold Pool, which are critical to focus those future studies on.

Conclusion

The MAB Cold Pool is a valuable coastal ocean feature that supports some of the most economically and culturally valuable fisheries in the USA. The Cold Pool influences a variety of oceanographic processes, such as atmospheric and oceanic circulation, coastal primary productivity, and carbon sequestration. Development of offshore wind has been rapidly expanding throughout the MAB. This study found that there is a notable overlap between proposed MAB offshore wind lease areas. In addition, substantial stratification persists past the time at which bottom temperatures warmed above Cold Pool thresholds. Bottom temperatures warm more rapidly in nearshore than offshore, despite stronger thermal gradients in nearshore sites. Although it is evident that MAB WLAs occur

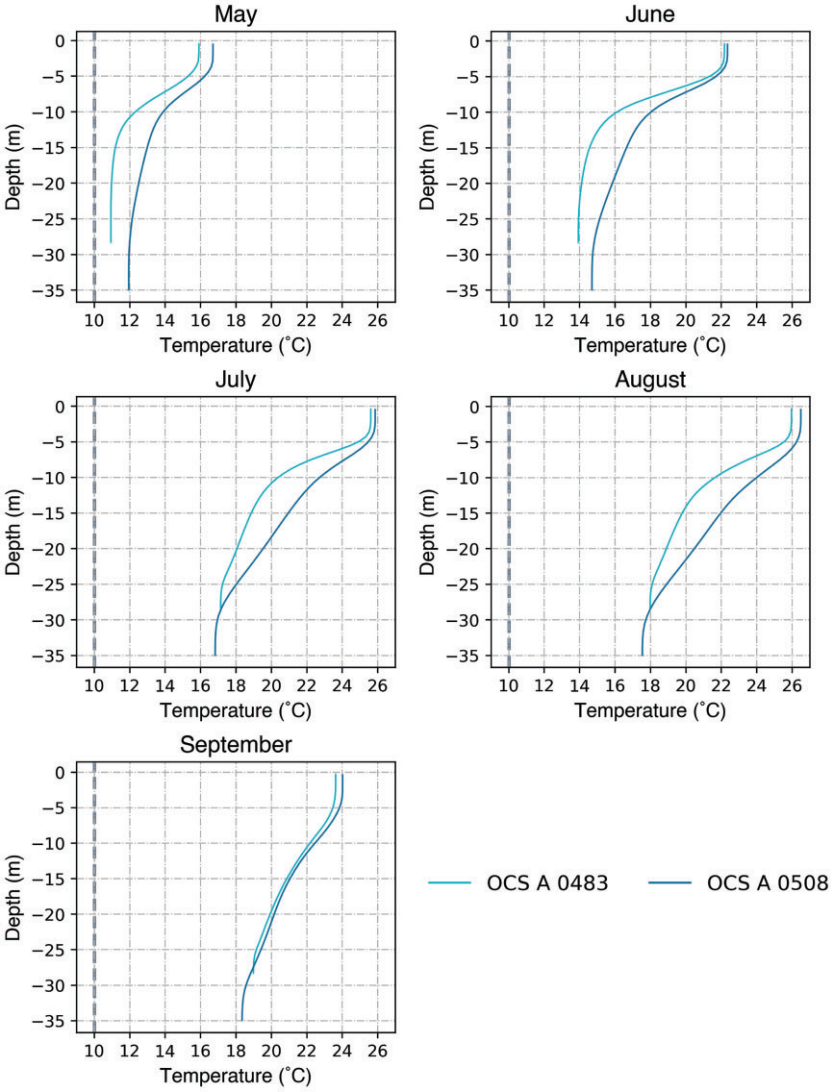

Figure 10. Southern MAB WLAs temperature profiles for Cold Pool months based on monthly averaged Doppio simulations from 2007 to 2021. Cold Pool bottom temperature threshold is depicted with the gray dashed line. The color of each profile corresponds to a study point within the selected wind areas shown in Fig. 1. The x-axis is not consistent with previous like figures (Figs 6 and 8) due to the warmer surface water temperatures within the southern MAB region.

within the Cold Pool, future studies to determine interdecadal trends of Cold Pool evolution and extent are necessary to further evaluate overlap between the Cold Pool and WLAs.

Acknowledgments

We thank the Rutgers University Department of Marine and Coastal Sciences and the Haskin Shellfish Research Lab at Rutgers University for their continued support. We also thank Julia Levin, John Wilkin, and Alex Lo`pez for their help with Doppio and for making their data publicly accessible. Special thanks to Joe Gradone, Jenn Gius, Laura Steeves, and Ailey Sheehan. Rebecca Horwitz was supported by the National Science Foundation Grant No. OCE-1831625, and this research was supported by the National Science Foundation Industry/University Cooperative Research Center SCeMFiS (Science Center for Marine Fisheries) NSF award #1841112. D.M. was partly supported by USDA NIFA Hatch project 1020831/NJ33140.

Conflict of interest: The authors have no competing interests to declare.

Data availability

Open data access for the Doppio model is described at SEANOE (https://www.seanoe.org/data/00785/89673) and was originally published in Wilkin and Levin (2022). Open GIS data access for the most up to date United States' wind lease areas can be found on The Bureau of Ocean Energy Management website (https://www.boem.gov/renewable-energy/mapping-and-data/renewable-energy-gis-data).

Author Contributions

DM and JK acquired funding; RH, TNM, DM, and JK conceived the ideas; RH and TNM developed methodology and contributed to data analysis; RH wrote model output analysis code and conducted overall data collection; RH drafted

initial manuscript and further incorporated additional analysis and edits from the review process; all authors contributed to manuscript review and editing.

References

Amaya DJ, Jacox MG, Alexander MA *et al.* Bottom marine heatwaves along the continental shelves of North America. *Nat Commun* 2023;**14**:1038. https://doi.org/10.1038/s41467-023-36567-0.

Bigelow HB. 1933. *Studies of the Waters on the Continental Shelf, Cape Cod to Chesapeake Bay*. Cambridge, MA: Massachusetts Institute of Technology and Woods Hole Oceanographic Institution. https://hdl.handle.net/1912/1144 (last accessed 10 June 2021).

BOEM. Renewable Energy GIS Data. 2023. https://www.boem.gov/renewable-energy/mapping-and-data/renewable-energy-gis-data (last accessed 10 Jul 2023).

Boyer, TP,, Antonov JI,, Baranova, OK,, Garcia, HE,, DR, Johnson,, Mishonov, AV,, O'Brien, TD *et al.* 2013. World Ocean Database 2013. U.S. Department of Commerce, National Oceanic and Atmospheric Administration, National Environmental Satellite, Data, and Information Service, National Oceanographic Data Center, Ocean Climate Laboratory. https://repository.library.noaa.gov/view/noaa/1291 (last accessed 30 August 2023).

Brown W, Boicourt W, Flagg C *et al.* Mapping the Mid-Atlantic Cold Pool evolution and variability with ocean gliders and numerical models. In: *2012 Oceans*, Hampton Roads, VA: IEEE, 2012. http://ieeexplore.ieee.org/document/6404970/ (last accessed 1 March 2022).

Brunner K, Lwiza KMM. Tidal velocities on the Mid-Atlantic Bight continental shelf using high-frequency radar. *J Oceanogr* 2020;**76**:289–306. https://doi.org/10.1007/s10872-020-00545-7.

Carpenter JR, Merckelbach L, Callies U *et al.* Potential impacts of offshore wind farms on North Sea stratification. *PLoS One* 2016;**11**:e0160830. Public Library of Science. https://doi.org/10.1371/journal.pone.0160830.

Castelao R, Glenn S, Schofield O. Temperature, salinity, and density variability in the central Middle Atlantic Bight. *J Geophys Res Oceans* 2010;**115**:2009JC006082. https://doi.org/10.1029/2009JC006082.

Chen Z, Curchitser E, Chant R *et al.* Seasonal variability of the cold pool over the Mid-Atlantic Bight continental shelf. *J Geophys Res Oceans* 2018;**123**:8203–26. https://doi.org/10.1029/2018JC014148.

Chen Z, Curchitser EN. Interannual variability of the Mid-Atlantic Bight Cold Pool. *J Geophys Res Oceans* 2020;**125**. https://onlinelibrary.wiley.com/doi/10.1029/2020JC016445 (last accessed 31 March 2023).

Christiansen N, Daewel U, Djath B *et al.* Emergence of large-scale hydrodynamic structures due to atmospheric offshore wind farm wakes. *Front Mar Sci* 2022;**9**:818501. https://doi.org/10.3389/fmars.2022.818501.

Daewel U, Akhtar N, Christiansen N *et al.* Offshore wind farms are projected to impact primary production and bottom water deoxygenation in the North Sea. *Commun Earth Environ* 2022;**3**:292. https://doi.org/10.1038/s43247-022-00625-0

de Boyer Montégut C, Madec G, Fischer AS *et al.* Mixed layer depth over the global ocean: an examination of profile data and a profile-based climatology. *J Geophys Res Oceans* 2004;**109**. https://onlinelibrary.wiley.com/doi/abs/10.1029/2004JC002378 (last accessed 1 March 2022).

Drévillon M, Bourdallé-Badie R, Derval C *et al.* The GODAE/Mercator-Ocean global ocean forecasting system: results, applications and prospects. *J Oper Oceanogr* 2008;**1**:51–7. https://doi.org/10.1080/1755876X.2008.11020095.

Egbert GD, Erofeeva SY. Efficient inverse modeling of barotropic ocean tides. *J Atmos Oceanic Technol* 2002;**19**:183–204. https://doi.org/10.1175/1520-0426(2002)019%3c0183:EIMOBO%3e2.0.CO;2.

Floeter J, Pohlmann T, Harmer A *et al.* Chasing the offshore wind farm wind-wake-induced upwelling/downwelling dipole. *Front Mar Sci* 2022;**9**:884943. https://doi.org/10.3389/fmars.2022.884943.

Friedland KD, Adams EM, Goetsch C *et al.* Forage fish species prefer habitat within designated offshore wind energy areas in the U.S. Northeast shelf ecosystem. *Mar Coast Fish* 2023;**15**:e10230. https://doi.org/10.1002/mcf2.10230.

Friedland KD, Miles T, Goode AG *et al.* The Middle Atlantic Bight Cold Pool is warming and shrinking: indices from in situ autumn seafloor temperatures. *Fish Oceanogr* 2022;**31**:217–23. https://doi.org/10.1111/fog.12573.

Gabriel WL. Persistence of demersal fish assemblages between Cape Hatteras and Nova Scotia, Northwest Atlantic. *J Northw Atl Fish Sci* 1992;**14**:29–46. https://doi.org/10.2960/J.v14.a2.

Glenn S, Arnone R, Bergmann T *et al.* Biogeochemical impact of summertime coastal upwelling on the New Jersey Shelf. *J Geophys Res Oceans* 2004;**109**. https://onlinelibrary.wiley.com/doi/abs/10.1029/2003JC002265 (last accessed 10 September 2022).

Glenn S, Schofield O. Observing the oceans from the COOL Room: our history, experience and opinions. *Oceanography* 2003;**16**:37–52,. https://doi.org/10.5670/oceanog.2003.07.

Glenn SM, Miles TN, Seroka GN *et al.* Stratified coastal ocean interactions with tropical cyclones. *Nat Commun* 2016;**7**:10887. https://doi.org/10.1038/ncomms10887.

Golbazi M, Archer CL, Alessandrini S. Surface impacts of large offshore wind farms. *Environ Res Lett* 2022;**17**:064021. https://doi.org/10.1088/1748-9326/ac6e49.

Haidvogel DB, Arango HG, Hedstrom K *et al.* Model evaluation experiments in the North Atlantic Basin: simulations in nonlinear terrain-following coordinates. *Dyn Atmos Oceans* 2000;**32**:239–81. https://doi.org/10.1016/S0377-0265(00)00049-X.

Houghton R, Schlitz R, Beardsley R *et al.* The Middle Atlantic Bight cold pool: evolution of the temperature structure during summer 1979. *Journal of Physical Oceanography* 1982;**12**:1019–29. https://doi.org/10.1175/1520-0485(1982)012⟨1019:TMABCP⟩2.0.CO;2.

Janjic Z, Black T, Pyle M *et al. High Resolution Applications of the WRF NMM*. Washington, DC. 2005. https://ams.confex.com/ams/WAFNWP34BC/techprogram/paper_93724.htm (last accessed 31 March 2023).

Lentz SJ. Seasonal warming of the Middle Atlantic Bight Cold Pool. *J Geophys Res Oceans* 2017;**122**:941–54. https://doi.org/10.1002/2016JC012201.

Li Y, Fratantoni PS, Chen C *et al.* Spatio-temporal patterns of stratification on the Northwest Atlantic shelf. *Prog Oceanogr* 2015;**134**:123–37. https://doi.org/10.1016/j.pocean.2015.01.003.

Li Y, Ji R, Fratantoni PS *et al.* Wind-induced interannual variability of sea level slope, along-shelf flow, and surface salinity on the Northwest Atlantic shelf. *J Geophys Res Oceans* 2014;**119**:2462–79. https://doi.org/10.1002/2013JC009385.

López AG, Wilkin JL, Levin JC. Doppio—a ROMS (v3.6)-based circulation model for the Mid-Atlantic Bight and Gulf of Maine: configuration and comparison to integrated coastal observing network observations. *Geosci Model Dev* 2020;**13**:3709–29. https://doi.org/10.5194/gmd-13-3709-2020.

Lucey S, Nye J. Shifting species assemblages in the Northeast US Continental Shelf large marine ecosystem. *Mar Ecol Prog Ser* 2010;**415**:23–33. https://doi.org/10.3354/meps08743.

Mesinger F, DiMego G, Kalnay E *et al.* North American Regional Reanalysis. *Bull Am Meteorol Soc* 2006;**87**:343–60. https://doi.org/10.1175/BAMS-87-3-343.

Methratta E, Hawkins A, Hooker B *et al.* Offshore wind development in the Northeast US Shelf large marine ecosystem: ecological, Human, and fishery management dimensions. *Oceanography* 2020;**33**:16–27. https://doi.org/10.5670/oceanog.2020.402.

Methratta ET, Silva A, Lipsky A *et al.* Science priorities for offshore wind and Fisheries research in the northeast U.S. Continental shelf ecosystem: perspectives from scientists at the National Marine Fisheries Service. *Mar Coast Fish* 2023;**15**:e10242. https://doi.org/10.1002/mcf2.10242.

Miles T, Murphy S, Kohut J *et al.* Offshore wind energy and the Mid-Atlantic Cold Pool: a review of potential interactions. *Mar Technol Soc J* 2021;**55**:72–87. https://doi.org/10.4031/MTSJ.55.4.8.

Mountain DG. Variability in the properties of Shelf Water in the Middle Atlantic Bight, 1977–1999. *J Geophys Res* 2003;**108**:3014. https://doi.org/10.1029/2001JC001044.

Munroe DM, Narváez DA, Hennen D *et al.* Fishing and bottom water temperature as drivers of change in maximum shell length in Atlantic surfclams (*Spisula solidissima*). *Estuar Coast Shelf Sci* 2016;**170**:112–22. https://doi.org/10.1016/j.ecss.2016.01.009.

Murray T. Economic activity associated with SCeMFiS supported fishery products (Ocean Quahog & Atlantic Surfclams). 2016. https://scemfis.org/wp-content/uploads/2020/02/Ec_Impact-tjm_rm2.pdf (last accessed 10 September 2022).

Musial W, Spitsen P, Duffy P *et al. Offshore Wind Market Report: 2022 Edition*. U.S Department of Energy. Office of Energy Efficiency and Renewable Energy. Washington, DC. 2022. DOE/GO-102022-5765. https://www.energy.gov/sites/default/files/2022-08/offshore_wind_market_report_2022.pdf (last accessed 10 September 2022).

Ou HW, Houghton R. A model of the summer progression of the cold-pool temperature in the Middle Atlantic Bight. *J Phys Oceanogr* 1982;**12**:1030–6. https://doi.org/10.1175/1520-0485(1982)012%3c1030:AMOTSP%3e2.0.CO;2.

Powell EN, Ewing AM, Kuykendall KM. Ocean quahogs (*Arctica islandica*) and Atlantic surfclams (*Spisula solidissima*) on the Mid-Atlantic Bight continental shelf and Georges Bank: the death assemblage as a recorder of climate change and the reorganization of the continental shelf benthos. *Palaeogeogr Palaeoclimatol Palaeoecol* 2020;**537**:109205. https://doi.org/10.1016/j.palaeo.2019.05.027.

Sackett D, Able K, Grothues T. Habitat dynamics of summer flounder paralichthys dentatus within a shallow USA estuary, based on multiple approaches using acoustic telemetry. *Mar Ecol Progr Ser* 2008;**364**:199–212. https://doi.org/10.3354/meps07391.

Shchepetkin AF, McWilliams JC. The regional oceanic modeling system (ROMS): a split-explicit, free-surface, topography-following-coordinate oceanic model. *Ocean Model* 2005;**9**:347–404. https://doi.org/10.1016/j.ocemod.2004.08.002.

Shields M, Marsh R, Stefek J *et al. The Demand for a Domestic Offshore Wind Energy Supply Chain*. Technical Report, NREL/TP-5000-81602. National Renewable Energy Laboratory (NREL), Denver, CO. 2022. https://www.nrel.gov/docs/fy22osti/81602.pdf (last accessed 10 September 2022).

Sullivan MC, Cowen RK, Steves BP. Evidence for atmosphere-ocean forcing of yellowtail flounder (*Limanda ferruginea*) recruitment in the Middle Atlantic Bight. *Fish Oceanogr* 2005;**14**:386–99. https://doi.org/10.1111/j.1365-2419.2005.00343.x.

van Berkel J, Burchard H, Christensen A *et al.* The effects of offshore wind farms on hydrodynamics and implications for fishes. *Oceanography* 2020;**33**:108–17. https://doi.org/10.5670/oceanog.2020.410.

Wallace E, Looney L, Gong D. Multi-decadal trends and variability in temperature and salinity in the Mid-Atlantic Bight, Georges Bank, and Gulf of Maine. *J Mar Res* 2018;**76**:163–215. https://doi.org/10.1357/002224018826473281.

Wilkin J, Levin J, Moore A *et al.* A data-assimilative model reanalysis of the U.S. Mid Atlantic Bight and Gulf of Maine: configuration and comparison to observations and global ocean models. *Prog Oceanogr* 2022;**209**:102919. https://doi.org/10.1016/j.pocean.2022.102919.

Wilkin J, Levin J. Outputs from a Regional Ocean Modeling System (ROMS) data assimilative reanalysis (version DopAnV3R3-ini2007) of ocean circulation in the Mid-Atlantic Bight and Gulf of Maine for 2007-2021. 2022. SEANOE. https://www.seanoe.org/data/00785/89673/ (last accessed 30 March 2023).

Xu Y, Chant R, Gong D *et al.* Seasonal variability of chlorophyll a in the Mid-Atlantic Bight. *Cont Shelf Res* 2011;**31**:1640–50. https://doi.org/10.1016/j.csr.2011.05.019.

Handling Editor: Steven Degraer